Observation and Rovibrational Analysis of the Intermolecular HCl Libration Band ν_4^1 in OC−HCl. Modeling of the Intermolecular Potential Energy Surface

R. Wugt Larsen,*,† F. Hegelund,‡ and B. Nelander†

Chemical Center, Department of Chemical Physics, Lund University, P.O. Box 124, S-221 00 Lund, Sweden, and Department of Chemistry, Aarhus University, Langelandsgade 140, DK-8000 Aarhus C, Denmark

Received: October 1, 2003; In Final Form: December 10, 2003

The high-resolution far-infrared spectrum of the intermolecular HCl libration band ν_4^1 of the OC−H^{35}Cl heterodimer is recorded in the gas phase by means of Fourier transform IR spectroscopy in a static multipass absorption cell at 137 K using a synchrotron radiation source. This is the first direct observation of an intermolecular vibration band of the OC−HCl dimer in the gas phase. The rotational structure of the band has the typical appearance of a perpendicular band of a linear polyatomic molecule. The structure is analyzed to yield the band origin $\nu_0 = 201.20464(27)$ cm^{-1} together with values for the upper state rotational constant, the upper state quartic and sextic centrifugal distortion constants, and the *l*-type doubling constant. The determined values for the rotational constant and the centrifugal distortion constants are used to obtain a Morse potential for the stretching of the intermolecular distance. The results are compared to the results from quantum-chemical calculations.

1. Introduction

To understand intermolecular interactions in general, and the hydrogen bond in particular, quantitative information on intermolecular interaction potentials for isolated hydrogen-bonded molecular complexes is very valuable. A direct source of such detailed information is the observation and rovibrational analyses of high-resolution infrared absorption spectra of molecular complexes in the gas phase. These absorption spectra may help to characterize the forces acting between the two molecular species, as well as how the intramolecular potentials within the units are modified by the incorporation into the bimolecular entity.

Experimentally, two complementary methods for investigating rotationally resolved infrared absorption spectra of molecular complexes have been dominating. In the first method, the molecular complexes are formed in a molecular beam from a supersonic expansion. The molecular complexes can be cooled to a very low temperature by means of collisionless expansion and therefore achieve a state in which no further reaction or decomposition is possible. The concentration of the molecular complexes, relative to monomers, is relatively large at these temperatures. This technique is very suitable for studies of weakly bound molecular complexes. The second method is the use of a long path length static absorption cell containing the molecular complexes in equilibrium with the monomers at low temperatures, the temperature being chosen to optimize the concentration of the molecular complex without causing condensation of the monomers present. Because the kinetic energy of the components must be less than or comparable to the electronic binding energy of the molecular complex at the equilibrium temperatures, this technique is mostly suitable for studies of stronger molecular complexes as those held together by hydrogen bonds.

A few decades ago the majority of experimental information on the structure of molecular complexes near the equilibrium conformation was provided from microwave (MW) studies of molecular beams. Nowadays, a variety of rotationally resolved far-IR, mid-IR, near-IR, and UV/VIS spectroscopic techniques have substantially outstriped the microwave efforts. The technique of a static cell containing equilibrium gas mixtures at low temperatures has complementary advantages. Whereas the molecular beam techniques have proven invaluable for determining equilibrium structures of complexes and the shape of the intermolecular potential energy surface near its minimum, the static cell spectra can give information of a larger part of the attractive portion of the intermolecular potential energy surface because, at the higher temperatures in the absorption cell, higher rotational and vibrational levels are populated. Far-infrared spectra give direct information about intermolecular potential surfaces. Despite this, only a few far-infrared studies of molecular complexes have been published possibly because the generally available light sources are rather poor in this spectral region.

In the present work, we characterize the intermolecular potential energy surface of the hydrogen-bonded molecular complex between CO and HCl by means of high-resolution Fourier transform far-infrared spectroscopy in a static absorption cell using a synchrotron radiation light source.

The first observation of the molecular complex between CO and HCl in the gas phase was reported by Soper et al.,[1] who used pulsed nozzle Fourier transform MW spectroscopy to obtain accurate ground-state spectroscopic constants, a ground-state molecular structure, and some estimates of intermolecular bending and stretching vibrations in the molecular complex. This work showed that the most stable complex between CO and HCl has a linear structure at equilibrium with the atom order OC−HCl, thus establishing the presence of a hydrogen bond to the carbon atom of the CO molecule. The vibrationally averaged distance between the centers of mass of the two monomers was determined to be 4.307 Å.

* To whom correspondence should be addressed. E-mail: wugt@larsen.dk.
† Lund University.
‡ Aarhus University.

10.1021/jp036935u CCC: $27.50
Published on Web 02/10/2004

The linear OC−HCl dimer has five modes of intermolecular vibrational motion: one stretch of the intermolecular hydrogen bond ν_3, a doubly degenerate high-frequency bending vibration ν_4^1 (libration of HCl), and a doubly degenerate low-frequency bending vibration ν_5^1 (libration of CO). In addition, the dimer has the intramolecular HCl and CO stretching vibrations ν_1 and ν_2. The molecular beam studies by Wang et al.[2] and F. Meads et al.[3] have provided the observation and assignment of the intramolecular bands ν_1 and ν_2 located at 2851.67 and 2155.50 cm^{-1}, respectively. The observed blue-shift of the ν_2 band relative to the fundamental band in the CO monomer of ca. 12.23 cm^{-1} indicates a weakening of the intermolecular hydrogen bond upon intramolecular vibrational excitation of the ν_2 vibration. The observed red shift of the ν_1 band relative to the HCl monomer fundamental band of -34.19 cm^{-1} indicates a stronger intermolecular hydrogen bond in the excited vibrational state $v_1 = 1$. Later McKellar et al.[4] reproduced these results by means of high-resolution gas-phase IR spectroscopy in a cooled static multipass cell. In this study, the higher temperature in a static cell was used to extend the line assignments to much higher J values, and extended centrifugal distortion parameters were determined for the ground state. The most recent spectroscopic gas phase study of the OC−HCl dimer was reported by R. Garnica et al.[5] In this work, the high-resolution near-infrared spectrum of the combination band $\nu_2 + \nu_5^1$ was recorded using high-frequency wavelength modulation diode laser supersonic jet spectroscopy. In addition, static gas-phase spectra of the associated $\nu_2 + \nu_5^1 - \nu_5^1$ and $\nu_2 + 2\nu_5^2 - 2\nu_5^2$ hot bands were observed. Garnica et al. managed to evaluate the band origin for the intermolecular low-frequency bending band ν_5^1 to be 48.99 cm^{-1} together with spectroscopic constants for the v_5 level from a combined rovibrational analysis of these bands.

The spectrum of the intermolecular high-frequency bending vibration band ν_4^1 of gas-phase OC−HCl has not yet been observed. This band is expected to have the largest transition moment of the intermolecular vibrations in the dimer owing to the significant change of the molecular dipole moment upon librational motion of the HCl molecule. In the MW study by Soper et al.,[1] the band origin of ν_4^1 was estimated to be 288 cm^{-1} from the observed value of the measured Cl nuclear quadrupole coupling constant. In an infrared matrix isolation study, Andrews et al.[6] observed a band at 247.1 cm^{-1} which was assigned to the ν_4^1 mode. We report here the direct observation and rovibrational analysis of the intermolecular HCl librational band ν_4^1 in gas-phase OC−HCl.

2. Experimental Details

The experiments were carried out at the infrared beam-line at MAX-Lab at Lund University. A temperature controlled 200-L static absorption cell made of stainless steel is interfaced with a Bruker IFS 120 HR Fourier transform spectrometer (FTS). The absorption cell has a White type multipass mirror system. The base length of the cell is 2.85 m, and the optics was aligned to give a total optical path length of ca. 91.2 m. The cell was equipped with two sets of 1.6 mm thick TPX windows. TPX has turned out to work well at least down to 130 K. A computer emulated PID temperature controller controls the current supplied to the three different resistive heaters welded to the outside of the inner cell and maintains the cell temperature within 0.25 K during an experiment. The cell temperature was kept at 137 K during the experiment, which is close to the condensation point of HCl. The partial pressures of HCl and CO in the cell were 6 and 20 hPa, respectively.

The light source was synchrotron radiation from the storage ring MAX-I at MAX-lab.[7,8] The storage ring is a high-brightness source of broadband infrared radiation, covering the full far-infrared spectral region. Synchrotron radiation is very close to a point source and is very suitable for high-resolution IR spectroscopy.[7−9] The interferometer was equipped with a 6 μm multilayer beam splitter during the measurements. The detector was a liquid He cooled Si bolometer operating at 1.8 K (Infared Laboratories, Inc.). The bolometer has been optimized for high-resolution studies. An appropriate high-transmission band-pass optical filter (0−370 cm^{-1}) was mounted in the bolometer in order to reduce the photonic noise level and detector nonlinearity effects in the final spectra. The combination of optical filtering from the bolometer, the 6 μm multilayer beam splitter, and the TPX cell windows give a band-pass in the region 50−370 cm^{-1}. The FTS instrument resolution (RES) is defined as $RES = 0.9/(MOPD)$, where MOPD is the maximum optical path difference in the interferometer. Sample interferograms were recorded with a resolution of 0.005 cm^{-1} (MOPD = 180 cm). The recorded sample interferograms were transformed using Mertz phase correction and boxcar apodization. A total scan time of ca. 12 h was achieved. The ultimate signal-to-noise ratio in the spectrum is limited not only by detector noise but also by the difficulty in recording precisely matched sample and background spectra. The raw spectra contain a number of interference fringes introduced by the various optical elements of the spectrometer, absorption cell, and transfer optics. Ideally these effects should be canceled out when ratioing the sample and background spectra. In reality this cancellation is seldom achieved due to drifts in the optics during recording of the spectra. In the present work, these effects were hard to control because of the low temperature of the absorption cell together with the large number of reflections in the absorption cell. For this reason, no high-resolution background spectrum was recorded. The background interferograms were recorded with a resolution of 0.08 cm^{-1}. These were transformed and interpolated onto a wavenumber grid matching that of the sample spectra using a zero-filling factor of 16. The background resolution proved to be appropriate in order to cancel out the most dominant interference fringes.

The absolute wavenumber scale of the spectra was that determined from a calibration of the internal FTS He−Ne laser. The accuracy of this calibration was checked by comparing line positions from H_2O in the spectra with literature values reported by Johns.[10] The water lines appear in our spectra owing to residual water vapor in the evacuated interferometer tank. The accuracy of these water line positions is estimated to be 0.0002 cm^{-1}.[10] Lists of line positions from the absorbance spectra were generated using the Microcal Origin 6.0 software package (Microcal software, Inc.). The precision of the line positions reported in the present study is estimated to be equal to the spectral resolution, that is, 0.005 cm^{-1}.

3. Rovibrational Analysis

The spectrum of the HCl libration band ν_4^1 of OC−HCl shows a Q branch at 201.2 cm^{-1} which degrades widely at lower wavenumbers. The Q branch is accompanied by weaker R and P branches; the R branch forming a band head near 203.1 cm^{-1}, whereas the P branch shows increasing J-spacing toward lower wavenumbers. This appearance is typical for a linear molecule perpendicular band with a rather large negative value for ΔB. This is to be expected for the motion associated with the libration mode in OC−HCl. The Q branch and the P branch are assigned to $J = 60$ and 32, respectively (Table 1). Figure 1 shows the Q

TABLE 1: Summary of the Assigned Line Positions for the ν_4^1 Band of OC−H^{35}Cl

transition	observed line position/ cm^{-1}	observed-calculated/ cm^{-1}	transition	observed line position/ cm^{-1}	observed-calculated/ cm^{-1}
P(2)	200.97798	−0.00065	Q(40)	198.66320	0.00101
P(4)	200.74001	−0.00079	Q(41)	198.52413	−0.00142
P(6)	200.49277	0.00161	Q(42)	198.38505	0.00047
P(7)	200.35988	−0.00203	Q(43)	198.23671	−0.00250
P(9)	200.09410	−0.00040	Q(44)	198.08837	−0.00097
P(13)	199.52236	−0.00157	Q(46)	197.77623	0.00044
P(14)	199.37401	0.00023	Q(47)	197.61243	0.00051
P(16)	199.06187	−0.00250	Q(48)	197.44245	−0.00075
P(17)	198.90426	−0.00082	Q(49)	197.26939	−0.00014
P(18)	198.74046	−0.00225	Q(50)	197.09014	−0.00066
P(19)	198.57666	−0.00058	Q(51)	196.90780	0.00088
P(20)	198.40978	0.00112	Q(52)	196.71928	0.00151
P(21)	198.23671	−0.00022	Q(53)	196.52149	−0.00175
P(23)	197.88439	0.00045	Q(54)	196.32369	0.00047
P(24)	197.70206	−0.00056	Q(55)	196.11972	0.00214
P(25)	197.51663	−0.00143	Q(56)	195.90648	0.00027
P(26)	197.33120	0.00099	Q(58)	195.46454	−0.00119
P(28)	196.94488	0.00033	Q(59)	195.23584	−0.00053
P(30)	196.54312	−0.00222	Q(60)	195.00096	0.00022
P(31)	196.34224	0.00169	R(0)	201.31175	−0.00145
P(32)	196.13208	−0.00019	R(1)	201.41683	−0.00197
Q(23)	200.38770	−0.00011	R(2)	201.52191	0.00049
Q(24)	200.31352	−0.00147	R(4)	201.71970	0.00197
Q(25)	200.23935	0.00054	R(5)	201.80932	−0.00206
Q(26)	200.15900	−0.00024	R(6)	201.90204	0.00001
Q(27)	200.07556	−0.00069	R(7)	201.99166	0.00201
Q(28)	199.98902	−0.00076	R(8)	202.07201	−0.00222
Q(29)	199.89940	−0.00039	R(9)	202.15546	−0.00030
Q(30)	199.80668	0.00045	R(12)	202.38415	0.00231
Q(31)	199.71088	0.00182	R(14)	202.51705	0.00012
Q(32)	199.60889	0.00068	R(15)	202.58195	0.00223
Q(33)	199.50381	0.00018	R(16)	202.64067	0.00137
Q(34)	199.39565	0.00037	R(18)	202.74883	0.00009
Q(36)	199.16695	−0.00002	R(19)	202.79828	−0.00025
Q(37)	199.04642	−0.00048	R(21)	202.88790	−0.00020
Q(38)	198.92280	0.00001	R(23)	202.96517	0.00109
Q(39)	198.79609	0.00151			

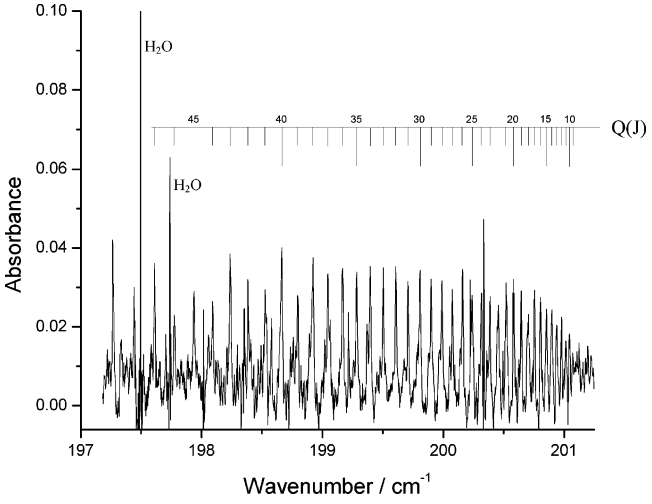

Figure 1. Portion of the absorbance spectrum of the ν_4^1 band of OC−H^{35}Cl in the spectral region of the Q branch. The numbered lines above the trace indicate the assigned Q(9) to Q(47) lines of the band (see Table 1).

branch assignment. For the R branch, a band head appears for $J = 32,33$. For this reason, assignments are only made up to $J = 23$ for this branch (Table 1). An additional number of weak absorption lines are observed in the Q-branch region, some of which probably belong to the OC−H^{37}Cl isotopologue and some which are likely to be hot band transitions in OC−H^{35}Cl. The presence of the hot band absorption lines, however, makes it very difficult to identify the Q branch of OC−H^{37}Cl. It is not possible to establish a final J assignment for these absorption lines.

A standard linear molecule model based on the rovibrational energy expressions in eqs 1 and 2[11] is used to fit values of the upper state spectroscopic constants B_1, D_J^1, and H_J^1. The ground-state constants B_0, D_J^0, and H_J^0 are constrained to the values obtained from the study by McKellar.[4]

$$E_0 = B_0 J(J+1) - D_J^0 J^2(J+1)^2 + H_J^0 J^3(J+1)^3 \quad (1)$$

$$E_1 = \nu_0 + B_1(J+1) - D_J^1 J^2(J+1)^2 + H_J^1 J^3(J+1)^3 \pm {}^1/_2(q + q_J J(J+1))J(J+1) \quad (2)$$

From separate analyses of the Q branch and the P, R branch system by this model, it appears that ΔB as obtained from the Q branch fit is numerically larger than ΔB as obtained from the P, R branch fit. This is an indication of the presence of l-type doubling, and we estimate the value of the l-type doubling constant q to be 3.43(17) × 10^{-5} cm^{-1}. Including l-type doubling in our model, we have analyzed the P-, Q-, and R-branch transitions simultaneously. The resulting spectroscopic constants are given in Table 2. In this fit, the ground-state constants are also constrained to the values obtained from McKellar.[4] A total number of 94 transitions are fitted with a standard deviation of 0.00123 cm^{-1} using a model including the sextic distortion constant H_J, the l-type doubling constant q, and its higher order correction term q_J.

TABLE 2: Spectroscopic Constants (in cm^{-1}) Obtained from the Rovibrational Analysis of the HCl Libration Band ν_4^1 of OC−H^{35}Cl[a]

ν_0	201.20464(27)[b]
ΔB	−0.0014631(13)
$10^7 \times \Delta D_J$	0.574(13)
$10^{11} \times \Delta H_J$	−0.221(15)
q	0.0000343(17)
$10^8 \times q_J$	−0.51(22)
N[c]	94
σ[d]	0.00123

[a] In the fit, the ground-state constants were fixed to the following values (4): $B_0 = 0.05576254$ cm^{-1}, $D_J^0 = 0.15686 \times 10^{-6}$ cm^{-1}, and $H_J^0 = -0.212 \times 10^{-11}$ cm^{-1} [b] Uncertainties quoted are one standard deviation. [c] Number of observations. [d] Standard deviation of fit (cm^{-1}).

In the complete treatment of Nielsen,[12,13] the *l*-type doubling constant is given by the following expression when $|l| = 1$:

$$2\frac{B_e^2}{\nu_4^1}\left(1 + 4\sum_i \frac{\xi_{4i}^2 (\nu_4^1)^2}{\nu_i^2 - (\nu_4^1)^2}\right) \quad (3)$$

where ν_i is a fundamental frequency in OC−HCl other than ν_4^1, and ξ_{4i} are the Coriolis coupling constants for the OC−HCl complex. These depend on the masses, dimensions, and harmonic force constants of the complex. In the following section, we estimate the hypothetical rotational constant B_e from observed and estimated vibration−rotation interaction constants. Together with estimates of the Coriolis coupling constants for the couplings between ν_4^1 and the stretching vibrations ν_1, ν_2, and ν_3 (the contribution from the Coriolis terms only makes up approximately 1%), we obtain a value of 3.23×10^{-5} cm^{-1} for the *l*-type doubling constant which almost reproduces the observed value within the uncertainty.

4. Modelling of the Intermolecular Stretching Potential Energy Surface from Spectroscopic Data

To characterize the intermolecular potential energy surface for the OC−HCl dimer using the spectroscopic data reported in the present work, we have constructed a model for the stretching of the intermolecular hydrogen bond in the dimer. The Schrödinger equation for a rotating linear complex between two linear molecules with an intermolecular Morse potential function is solved in order to relate the parameters of the Dunham expansion (the equilibrium values of the rotational constant B and the centrifugal distortion parameters D_J and H_J) to the Morse potential parameters D (the dissociation energy for the molecular complex), a (a constant defining the steepness of the potential energy surface), and r_e (the value of the center of mass distance). The relations between the Dunham coefficients and the Morse potential parameters are shown in the appendix.

A set of preliminary Morse potential parameters can be calculated for a given vibrational level according to eqs A6−A8 once the spectroscopic constants B, D_J, and H_J are known for that particular vibrational state. The spectroscopic constants have to be corrected for the vibrational dependencies in order to obtain the correct set of Morse potential parameters. We are able to calculate the intermolecular harmonic stretching frequencies, the anharmonicity constants, and the vibration−rotation interaction constants α_e and β_e according to eqs A9−A12 from the preliminary set of Morse potential parameters. The values of the vibration−rotation interaction constants α_e and β_e are used to correct for the dependency on the intermolecular stretching vibration of the experimental values of B and D_J. The corrected spectroscopic constants are then used to calculate improved values for the vibration−rotation interaction constants. This procedure is repeated iteratively until the values of the Morse potential parameters converge. The converged Morse potential parameters for the different HCl libration states together with the converged intermolecular harmonic stretching frequencies, the anharmonicity constants, and the vibration−rotation interaction constants α_e and β_e are listed in Table 3. The converged value of α_e only describes the vibrational dependence on B of the intermolecular stretching frequency ν_3. However, together with the observed vibration−rotation interaction constants for the other vibrational modes in OC−HCl reported in (2−5), we can estimate a value for the hypothetical equilibrium rotational constant B_e according to

TABLE 3: Morse Parameters, Harmonic Intermolecular Stretching Frequencies, Anharmonicity Constants, and Vibration−Rotation Interaction Constants for the Intermolecular Stretching Potential Determined from the Spectroscopic Constants and the Relations between Coefficients in the Dunham Expansion and the Morse Potential Parameters

Parameter	$\nu_4 = 0$	$\nu_4 = 1$
r_e/Å	4.2670	4.3157
a/Å^{-1}	1.8679	1.9709
D/cm^{-1}	313.3	195.9
ν_e/cm^{-1}	68.4	57.1
$\nu_e x_e$/cm^{-1}	3.736	4.159
α_e/cm^{-1}	1.98×10^{-3}	2.45×10^{-3}
β_e/cm^{-1}	1.22×10^{-8}	2.29×10^{-8}

$$B_e = B_0 + \sum_i \alpha_i g_i \quad (4)$$

where α_i is the vibration−rotation interaction constants for the ith fundamental vibration of OC−HCl and g_i is one-half of the corresponding degeneracy of the vibration. The equilibrium value for the rotational constant is used to estimate the center of mass distance r_{cm} at the equilibrium configuration of the molecular complex according to

$$r_{cm}^e = \sqrt{\frac{I_e^{OC-HCl} - I_e^{HCl} - I_e^{CO}}{\mu_{OC-HCl}}} \quad (5)$$

where μ_{OC-HCl} is the reduced mass of the OC−HCl complex. We find the center of mass distance r_{cm} at equilibrium to be 4.244 Å using the equilibrium bond lengths of CO and HCl.[14] The estimated equilibrium value of r_{cm} seems very reasonable compared to the vibrationally averaged distance of 4.307 Å estimated by Soper et al.[1] taking into consideration the expected effect of vibrational averaging. The contribution of vibrational averaging to a hydrogen bond length of ca. 0.05 Å has been reported for several other hydrogen bonded molecular complexes.[15,16]

The observed band center of the ν_4^1 mode gives direct information on the amplitudes of the internal rotation of the HCl molecule during the librational motion. The classical amplitude of the HCl libration angle θ_{HCl} changes from 18.5° in the vibrational ground state to 26.1° in the first excited HCl librational state.

The observed negative shift of ΔB together with the observed positive shift of ΔD_J is consistent with a significant weakening of the hydrogen bond in OC−HCl upon excitation of the HCl libration mode ν_4^1. The hydrogen bond elongates by 0.049 Å upon excitation of ν_4^1 according to the determined values of the

TABLE 4: Computed and Experimental Equilibrium Structural Parameters (in Å) of CO, HCl, and OC−HCl

	CO	HCl	OC−HCl			
	r_{CO}	r_{HCl}	r_{CO}	r_{HCl}	r_{CH}	r_{cm}
CCSD(T)/ aug-cc-pVTZ	1.136	1.279	1.134	1.283	2.365	4.267
exp	1.128[a]	1.275[a]				4.244[b]

[a] Reference 14. [b] From the empirical model presented in this work.

Morse potential parameter r_e. The empirical model estimates the intermolecular harmonic stretching frequency for the ground state to be 68.4 cm^{-1}. This value is close to the harmonic value of 67.5 cm^{-1} estimated by the modified pseudodiatomic (MPD) approximation.[17] The empirical model estimates the intermolecular harmonic stretching frequency to decrease to 57.1 cm^{-1} upon excitation of the HCl libration, a measure of the weakening of the hydrogen bond. The OC−HCl dimer is weakened by 117 cm^{-1} upon excitation of the ν_4^1 vibration according to the determined values of the Morse parameter D_e. However, the estimated Morse dissociation energies are expected to be of low accuracy because the precision of the observed higher order centrifugal distortion constants D_J and H_J is not very high.

5. Quantum-Chemical Calculations

5a. Equilibrium Configuration of OC−HCl. Standard ab initio molecular orbital theory[18] calculations are carried out using the program package Gaussian 98.[19] Geometry optimization procedures are performed for CO, HCl, and OC−HCl using MP2[20] and CCSD(T)[21] theory in combination with correlation consistent polarized valence double, triple-, and quadruple-ζ basis sets with and without the augmentation of additional diffuse functions.[22] Additional single-point energy calculations on selected dimer geometries are performed in order to calculate BSSE corrections. Harmonic vibrational frequency analyses are performed using the MP2 level of theory combined with the same basis sets. The results from the CCSD(T)/aug-cc-pVTZ level of theory are given in this paper, and the results from the other calculations are available from the authors on request.

In Table 4, the computed structural parameters obtained for CO, HCl, and OC−HCl at the CCSD(T)/aug-cc-pVTZ level of theory are compared with corresponding experimental geometries. The predicted bond lengths are in close agreement with experimental data for both of the monomers CO and HCl. The center of mass distance at equilibrium for the dimer is predicted to be 4.267 Å, assuming the monomer structures to be unchanged during the dimer formation. This assumption seems to be valid since the CCSD(T)/aug-cc-pVTZ level of theory predicts the H−Cl bond length to elongate by only 0.0036 Å and the C═O bond length to contract by only 0.002 Å upon the complex formation. In this study, we estimate an empirical value of r_{cm} for the equilibrium configuration to be 4.246 Å (see the previous section) in fairly nice agreement with the CCSD(T)/aug-cc-pVTZ value. The CCSD(T)/aug-cc-pVTZ level of theory thus seems to be reliable in the description of the OC−HCl structure. Consequently, the CCSD(T)/aug-cc-pVTZ level of theory is expected to give a reasonable value for the electronic binding energy for the formation of the dimer as well.

The calculated electronic equilibrium binding energy for the OC−HCl dimer is −654 cm^{-1} when corrected for the BSSE (177 cm^{-1}) being assessed using the Counterpoise (CP) correction as suggested by Boys & Bernadi.[23] The basis set limit has not been reached for the CCSD(T)/aug-cc-pVTZ level of theory. To estimate the basis set limit, we use the results of Dunning,[24] who has studied the basis set limit for CCSD(T) calculations of D_e for the hydrogen-bonded dimers $(H_2O)_2$ and $(HF)_2$ using correlation consistent basis sets. In this work, the BSSE corrected values of D_e for $(H_2O)_2$ and $(HF)_2$ were calculated using the CCSD(T) level of theory in combination with the aug-cc-pVnZ basis sets, $n = 1-4$. The conclusion of this work was that the basis set convergence errors for $(H_2O)_2$ and $(HF)_2$ for a specific basis set are very similar. For $(H_2O)_2$, the CCSD(T)/aug-pVTZ level of theory yields 94% of the complete basis set limit. Assuming this to be true also for the OC−HCl system, we predict an electronic equilibrium binding energy D_e of −696 cm^{-1} in the complete basis set limit.

TABLE 5: Harmonic Frequencies (cm^{-1}) Computed for HCl, CO, and OC−HCl at the MP2/cc-pVQZ Level of Theory and Experimental Gas Phase Frequencies

method	ν_5^1	ν_3	ν_4^1	ν_2	ν_1	ν_{CO}	ν_{HCl}
MP2/cc-pVQZ	65	86	312	2142	2972	2128	3050
exp	49[a]	(68)[ab]	201[ab]	2155[ac]	2852[ad]	2143[ae]	2886[ae]

[a] Reference 5. [b] This work. [c] References 2−4. [d] References 3 and 4. [e] The HITRAN molecular spectroscopic database.[25]

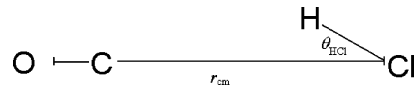

Figure 2. Illustration of the two structural parameters r_{cm} (the center of mass separation of HCl and CO) and θ_{HCl} (the HCl libration angle) which are used to describe the geometry of the molecular complex OC−HCl.

The harmonic frequency analysis at the MP2/cc-pVQZ level of theory yields a ZPE contribution of 388 cm^{-1} for the electronic binding energy (see Table 5). However, with the present study of the ν_4^1 band, all of the vibrational frequencies of the OC−HCl dimer in the gas phase have been determined experimentally (see Table 5) except for the weak intermolecular stretching band. We use the harmonic frequency of 68.4 cm^{-1} and the corresponding anharmonicity constant of 3.736 cm^{-1} estimated from our empirical model to estimate the zero point energy for this intermolecular stretching mode. This allows us to calculate an empirical ZPE contribution for the dimer of 274 cm^{-1} leading to an estimate of the electronic binding energy D_0 of −422 cm^{-1}.

5b. Potential Energy Surface Away from the Equilibrium Configuration. To give rough estimates of the spectroscopic constants and how these constants change upon the HCl librational motion, we have computed the interaction energy between CO and HCl on a two-dimensional grid of points at the CCSD(T)/aug-cc-pVTZ level of theory.

The angle θ_{HCl} defining the internal rotation of the HCl molecule around its center of mass is varied from 0° to 30° in steps of 10° and the distance r_{cm} between the centers of mass of the two monomers from 4.10 to 4.40 Å in steps of 0.05 Å (see Figure 2). The CO and HCl bond lengths are kept fixed at their computed equilibrium values. The CO monomer is directed toward the center of mass of the HCl molecule.

We assume a Born Oppenheimer type separation between the HCl libration and the center of mass stretch. For each value of the center of mass distance r_{cm}, the computed interaction energies for the different values of the angle θ_{HCl} are fitted to a fourth-order polynomial. It is assumed that the intermolecular potential energy surface is symmetric around r_{cm} so that seven grid points ($\theta_{HCl} = 0°$, ±10°, ±20°, and ±30°) are used for each value of r_{cm}. These polynomials are then used to calculate the energies of the three lowest libration states. The experimental B value of ground-state HCl is used. The contribution from the

TABLE 6: Intermolecular Harmonic Stretching Frequencies, Libration Frequencies, Rotational Constants, Centrifugal Distortion Constants, Equilibrium Dissociation Energies, and Equilibrium Center of Mass Separations in OC−HCl as Obtained from the CCSD(T)/Aug-cc-pVTZ Level of Theory and the Empirical Model

	CCSD(T)/aug-cc-pVTZ	experimental
ν_3/cm^{-1}	77.0	68.4[a]
($\upsilon_3 = 1$, $\upsilon_4 = 1$) ← ($\upsilon_3 = 0$, $\upsilon_4 = 1$)/cm^{-1}	64.7	57.1[a]
ν_4^1/cm^{-1}	243.7	201.2
B_0/cm^{-1}	0.05550	0.05576254
B_1/cm^{-1}	0.05396	0.054299
D_J^0/cm^{-1}	1.18×10^{-7}	1.5686×10^{-7}
D_J^1/cm^{-1}	1.59×10^{-7}	2.14×10^{-7}
H_J^0/cm^{-1}	-9.51×10^{-13}	-2.12×10^{-12}
H_J^1/cm^{-1}	-2.11×10^{-12}	-4.33×10^{-12}
D_e/cm^{-1}	654	325[a]
r_e/Å	4.267	4.246[b]
Δr_e/Å	−0.053	−0.054[a]

[a] Results from the empirical model described in Section 4. [b] Equation 5 (see section 4).

fourth degree term in the potential is obtained from first-order perturbation theory. Three different potential energy curves for r_{cm} are obtained from these calculations. The first r_{cm} curve goes through the minima of the libration potential curves, giving the energy of the hypothetical equilibrium state. The other two curves give the energies of the librational ground state and the lowest HCl libration excited state, respectively. These are obtained by addition of the respective libration energy to the energy at the minimum of the libration potential at the given r_{cm} with $\theta_{HCl} = 0$. Morse potential curves are then fitted to the four r_{cm} potential curves and from the solutions to the center of mass vibration for these potentials, we obtain estimates of the libration transition energy, the intermolecular harmonic stretching frequencies, and the centrifugal distortion constants of the two lowest libration states using the equations listed in the appendix. The calculated values are given in Table 6.

The theoretical values for the rotational constants and the intermolecular harmonic stretching frequencies in the different HCl libration states are close to the values obtained from the empirical model. The predicted values for the rotational constants agree within 0.6% of the experimental values. It must be noted that the calculations are made for the CO molecule fixed at its equilibrium orientation while the empirical potential is obtained for a vibrational average of the CO orientation. The calculations are therefore expected to give a somewhat higher interaction energy than the empirical potential. No BSSE corrections are applied to the calculated energies. The BSSEs are expected to decrease with increasing center of mass distance; we therefore expect the calculations to overestimate the energy variation with distance to some extent. We note that the quantum-chemical calculations predict the rotational constant to decrease ca. 2.9% upon excitation of the HCl libration mode which is close to the observed decrease of ca. 2.7%. The predicted values for the intermolecular harmonic stretching frequencies are approximately 12% larger than the values obtained from our empirical model. The quantum-chemical calculations predict the decrease of the intermolecular harmonic stretching frequency to be ca. 16%, from 77.0 cm^{-1} in the vibrational ground state to 64.7 cm^{-1} in the first excited HCl libration state, whereas the empirical model gives a decrease of 17%.

With respect to the centrifugal distortion constants D_J and H_J, the agreement between theory and experiment is less conspicuous. The absolute values of the quartic centrifugal distortion constants are predicted ca. 25% smaller than the observed ground state and upper state values possibly because the calculations overestimate the interaction energy. However, both experiment and theory show an increase of the D_J constant of ca. 35% upon the HCl librational motion. The predicted values of the sextic centrifugal distortion constants H_J have the same order of magnitude as the empirical values. The ab initio calculations predict the value of this constant to decrease upon excitation of ν_4^1 which is also confirmed by the rovibrational analysis.

The discrepancy between the predicted and observed HCl libration frequency may be due to both the lack of the BSSE correction and the fact that CO was kept at its equilibrium orientation.

6. Conclusions

The spectrum of the intermolecular ν_4^1 high-frequency bending mode in gas-phase OC−HCl is recorded using the high-brightness infrared radiation from the MAX-I storage ring at MAX-lab. A rovibrational analysis of the ν_4^1 band yields spectroscopic constants for the upper HCl librational state which are used to construct a model for the stretching of the intermolecular hydrogen bond in the dimer. The empirical model is in good agreement with results from CCSD(T) theory combined with the correlation-consistent aug-cc-pVTZ basis set indicating that this level of theory gives a rather accurate description of the molecular complex.

Acknowledgment. The running costs of the infrared beamline at MAX-lab are supplied by the Swedish National Science Council. The authors acknowledge the LUNARC center at Lund University the generous allocation of computer time on the Origin 2000 system from Silicon Graphics. R.W.L. acknowledges receipt of a three months stipend from MAX-lab and a travel grant from the Nordic Network for Chemical Kinetics (NoNeCK).

Appendix

Centrifugal Distortion Parameters of a Linear Complex between Two Linear Molecules with an Intermolecular Morse Potential. The vibrational Hamiltonian of the complex between two linear molecules is given by

$$\hat{H} = \left[-\frac{h^2}{8\pi^2\mu}\frac{1}{r}\left(\frac{\partial}{\partial r}\right)^2 r + D[1 - \exp(-a(r - r_e))]^2 + \frac{h^2}{8\pi^2}\frac{J(J+1) - l^2}{(I_1 + I_2 + \mu r^2)}\right] \quad \text{(A1)}$$

I_1 and I_2 are the moments of inertia of the two molecules. D, a, and r_e are the Morse potential parameters and μ is the reduced mass: $\mu = M_A M_B/(M_A + M_B)$ where M_A and M_B are the masses of the two molecules and r is the distance between the centers of mass of the two molecules. We introduce the Morse variable ζ

$$\zeta = \exp(-a(r - r_e)) \quad \text{(A2)}$$

and expand

$$\frac{h^2}{8\pi^2}\frac{J(J+1) - l^2}{I_1 + I_2 + \mu r^2} \quad \text{(A3)}$$

as

$$\frac{R}{I+\mu r^2} = A + B\zeta + C\zeta^2 \tag{A4}$$

where $I = I_1 + I_2$ and $R = (J(J+1) - l^2)h^2/(8\pi^2)$. Both sides of eq A4 are expanded in powers of $(r - r_e)$ up to and including $(r - r_e)^2$. This determines A, B, and C.

When these substitutions are made in eq A1, the resulting Hamiltonian has the same form as the standard Hamiltonian for a diatomic molecule with a Morse potential. The energy levels are given by

$$E_n = D + A - \frac{(2D-B)^2}{4(D-C)} + \left(n+\frac{1}{2}\right)\sqrt{\frac{h^2a^2}{8\pi^2\mu\sqrt{D+C}}}\,\frac{2D-B}{} - \left(n+\frac{1}{2}\right)^2\frac{h^2a^2}{8\pi^2\mu} \tag{A5}$$

A, B, and C are significantly smaller than D. By expanding and identification of coefficients, we obtain the following expressions for the spectroscopic constants:

$$B_e = \frac{h}{8\pi^2 cI + \mu r_e^2} \tag{A6}$$

$$D_e = \frac{h^3}{64\pi^4 c}\,\frac{\mu^2 r_e^2}{Da^2(I+\mu r_e^2)^4} \tag{A7}$$

$$H_e = \frac{h^5}{512\pi^6 c}\,\frac{1}{D^2a^4}\,\frac{\mu^3 r_e^2}{(I+\mu r_e^2)^6}\left(\frac{4\mu r_e^2}{I+\mu r_e^2} - 1 - r_e a\right) \tag{A8}$$

$$\omega_e = \sqrt{\frac{Da^2}{2\pi^2 c^2 \mu}} \tag{A9}$$

$$\omega_e x_e = \frac{ha^2}{8\pi^2 c\mu} \tag{A10}$$

$$\alpha_e = \frac{1}{hc}\frac{h^2}{8\pi^2}\sqrt{\frac{h^2a^2}{8\pi^2\mu\sqrt{D}}}\,\frac{1}{(I+\mu r_e^2)^3}\,\frac{\mu}{a^2}\,\frac{1}{\mu r_e^2}\left[3r_e a - 3 + \frac{I}{\mu r_e^2}\{1 + 3r_e a\}\right] \tag{A11}$$

$$\beta_e = \frac{2B_e^4}{\omega_e^3}\left(\frac{4\mu r_e^2}{I+\mu r_e^2} - 1 - r_e a\right)\left(5r_e a + 1 - \frac{4\mu r_e^2}{I+\mu r_e^2}\right) \tag{A12}$$

References and Notes

(1) Soper, P. D.; Legon, A. C.; Flygare, W. H. *J. Chem. Phys.* **1981**, *74*, 2138−2142.

(2) Wang, Z.; Eliades, M.; Bevan, J. W. *Chem. Phys. Lett.* **1989**, *161*, 6−1.

(3) Meads, R. F.; Hartz, C. L.; Lucchese, R. R.; Bevan, J. W. *Chem. Phys. Lett.* **1993**, *206*, 488−492.

(4) McKellar, A. R. W.; Lu, Z. *J. Mol. Spectrosc.* **1993**, *161*, 542−551.

(5) Garnica, R.; McIntosh, A. L.; Wang, Z.; Lucchese, R. R.; Bevan, J. W.; McKellar, A. R. *Chem. Phys. Lett.* **1997**, *272*, 484−488.

(6) Andrews, L.; Arlinghaus, R. T.; Johnson, G. L. *J. Chem. Phys.* **1983**, *78*, 6347.

(7) Nelander, B. *Vib. Spectrosc.* **1995**, *9*, 29.

(8) Johnson, M. S.; Nelander, B. *Il Nuovo Cimento* **1998**, *20*, *4*, 449.

(9) Duncan, W. D.; Williams, G. P. *Appl. Opt.* **1983**, *22*, 2914.

(10) Johns, J. W. C. *J. Opt. Soc. Am. B* **1985**, *2*, 1340−1354.

(11) Papousek, D.; Aliev, M. R. *Molecular Vibrational−Rotational Spectra: Theory and Applications of High-Resolution Infrared, Microwave and Raman Spectroscopy of Polyatomic Molecules*; Elsevier: Amsterdam, 1982.

(12) Nielsen, H. H. *Phys. Rev.* **1949**, *75*, 1961.

(13) Nielsen, H. H. *Rev. Mod. Phys.* **1951**, *23*, 90−136.

(14) Harmony, M. D. In *Equilibrium Structural Parameters*; Durig, J. R., Ed.; Elsevier: Amsterdam, 2000; pp 16−19.

(15) Hilpert, G.; Fraser, G. T.; Pine, A. S. *J. Chem. Phys.* **1996**, *105*, 6183−6191.

(16) Hartmann, M.; Radom, L. *J. Phys. Chem. A* **2000**, *104*, 968.

(17) Millen, D. J. *Can. J. Chem.* **1985**, *63*, 1477.

(18) Hehre, W. J.; Radom, L.; Schleyer, P. V. R.; Pople, J. A. *Ab Initio Molecular Orbital Theory*; Wiley: New York, 1986.

(19) Frisch, M. J.; Trucks, G. W.; Schlegel, H. B.; Scuseria, G. E.; Robb, M. A.; Cheeseman, J. R.; Zakrzewski, V. G.; Montgomery, J. A., Jr.; Stratmann, R. E.; Burant, J. C.; Dapprich, S.; Millam, J. M.; Daniels, A. D.; Kudin, K. N.; Strain, M. C.; Farkas, O.; Tomasi, J.; Barone, V.; Cossi, M.; Cammi, R.; Mennucci, B.; Pomelli, C.; Adamo, C.; Clifford, S.; Ochterski, J.; Petersson, G. A.; Ayala, P. Y.; Cui, Q.; Morokuma, K.; Malick, D. K.; Rabuck, A. D.; Raghavachari, K.; Foresman, J. B.; Cioslowski, J.; Ortiz, J. V.; Stefanov, B. B.; Liu, G.; Liashenko, A.; Piskorz, P.; Komaromi, I.; Gomperts, R.; Martin, R. L.; Fox, D. J.; Keith, T.; Al-Laham, M. A.; Peng, C. Y.; Nanayakkara, A.; Gonzalez, C.; Challacombe, M.; Gill, P. M. W.; Johnson, B. G.; Chen, W.; Wong, M. W.; Andres, J. L.; Head-Gordon, M.; Replogle, E. S.; Pople, J. A. *Gaussian 98*, revision A.5; Gaussian, Inc.: Pittsburgh, PA, 1998.

(20) Møller, C.; Plesset, M. S. *Phys. Rev.* **1934**, *46*, 618.

(21) Raghavachari, K.; Trucks, G. W.; Pople, J. A.; Head-Gordon, M. *Chem. Phys. Lett.* **1989**, *157*, 1007.

(22) Dunning, T. H. *J. Chem. Phys.* **1989**, *90*, 1007−1023, Woon, D. E.; Dunning, T. H. *J. Chem. Phys.* **1995**, *103*, 4572−4585. Kendall, R. A.; Dunning, T. H.; Harrison, R. J. *J. Chem. Phys.* **2000**, *96*, 6796−6806.

(23) Boys, S. F.; Bernadi, F. *Mol. Phys.* **1970**, *19*, 553.

(24) Dunning, T. H. *J. Phys. Chem. A* **2000**, *104*, 9062−9080.

(25) The HITRAN Molecular Spectroscopic Database. Rothman, L. S.; Barbe, A.; Benner, D. C.; Brown, L. R.; Camy-Peyret, C.; Carleer, M. R.; Chance, K.; Clerbaux, C.; Dana, V.; Devi, V. M., et al., *JQSRT* **2003**, *82*, 5.